



DETERMINATION OF THE SOLUBILIZING CHARACTER OF 1-METHOXYETHYL-1-METHYLPYRROLIDIUM TRIS(PENTAFLUOROETHYL)TRIFLUOROPHOSPHATE BASED ON THE ABRAHAM SOLVATION PARAMETER MODEL

**Pamela Twu^[a], Jared L. Anderson^[a], Timothy W. Stephens^[b], William E. Acree, Jr.^{[b]*}, and
Michael H. Abraham^[c]**

Keywords: chromatographic retention factors, partition coefficients, linear free energy relationships, ionic liquids

Chromatographic retention data were measured for a chemically diverse set of organic solutes on an anhydrous 1-methoxyethyl-1-methylpyrrolidinium tris(pentafluoroethyl)trifluorophosphate, ([MeoeMPip]⁺[FAP]⁻), stationary phase at both 323 K and 353 K. The experimental retention factors were combined with previously published thermodynamic data and gas-to-water partition coefficient data to yield gas-to-anhydrous ionic liquid (IL) and water-to-anhydrous IL partition coefficients. The three sets of partition coefficient data were analyzed in accordance with the Abraham model. The Abraham model correlations that were determined in the present study describe the observed gas-to-([MeoeMPip]⁺[FAP]⁻) (log *K*) and water-to-([MeoeMPip]⁺[FAP]⁻) (log *P*) partition coefficient data to within average standard deviations of approximately 0.13 and 0.16 log units, respectively.

* Corresponding Author
Fax: 1-940-565-4318
E-Mail: Bill.Acree@unt.edu

[a] University of Toledo, United States
[b] University of North Texas, United States
[c] University College London, United Kingdom

1. Introduction

Ionic liquids (ILs) have garnered considerable attention in recent years as potential “green solvent” replacements for the more traditional molecular organic solvents in applications involving chemical syntheses and chemical separations. Most (if not all) of the classic synthetic methods have been performed in ILs. Published studies have reported that much higher isolated product yields can be obtained in ILs with reduced reactions.¹⁻⁴ For select chemical reactions the IL may serve as both the reaction solvent media and catalyst, and the fact that many ionic liquids are immiscible with water and nonpolar organic solvents affords a convenient extraction method for separating the desired product(s) from any unreacted starting material(s). Ionic liquid have also been utilized as stationary phases in gas-liquid chromatography (glc)⁵⁻⁷ and high-performance liquid chromatography (hplc),^{8,9} and as sorbent materials for solid-phase microextractions.^{9,10} The fore-mentioned applications are facilitated by the ionic liquid’s unique physical and solubilizing properties, which are determined largely by the specific cation-anion pair combination. The large number of known (and possible) combinations provides a large list of ILs having different viscosity, thermal stability, polarity, water immiscibility and solubilizing characteristics. At present more than 500 different ionic liquids are known.

The solvation parameter model, developed by Abraham and coworkers^{11,12} has been successfully employed to evaluate the solubilizing properties of a large number of traditional organic solvents,¹³⁻¹⁸ and several classes of ILs containing 1,3-dialkylimidazolium, 1,1-dialkylpyrrolidinium, N-alkylpyridinium and tetraalkylammonium cations with both ionic and organic anions.¹⁹⁻³⁴ The solvation parameter model is based on two linear free energy relationships (LFERs), the first mathematical relationship governs solute transfer between two condensed phases

$$\log P = c_p + e_p \cdot E + s_p \cdot S + a_p \cdot A + b_p \cdot B + v_p \cdot V \quad (1)$$

while the second relationship describes solute transfer from the gas phase to a condensed phase

$$\log K = c_k + e_k \cdot E + s_k \cdot S + a_k \cdot A + b_k \cdot B + l_k \cdot L \quad (2)$$

The two dependent solute properties, *P* and *K*, refer to the condensed phase-to-condensed phase partition coefficient (often water-to-organic solvent partition coefficient) and gas-to-condensed phase partition coefficient of the solute, respectively. Mathematical equations describing the respective standard Gibbs energies of transfer, $\Delta G_{\text{water-to-organic solvent}}$ and $\Delta G_{\text{gas-to-organic solvent}}$ are obtained by multiplying log *K* and log *P* by $-2.303 RT$:

$$\begin{aligned} \Delta G_{\text{water-to-organic solvent}} &= -2.303 RT \log P \\ &= -2.303 RT (c_p + e_p \cdot E + s_p \cdot S + a_p \cdot A + b_p \cdot B + v_p \cdot V) \quad (3) \end{aligned}$$

$$\begin{aligned} \Delta G_{\text{gas-to-organic solvent}} &= -2.303 RT \log K \\ &= -2.303 RT (c_k + e_k \cdot E + s_k \cdot S + a_k \cdot A + b_k \cdot B + l_k \cdot L) \quad (4) \end{aligned}$$

For ionic liquid solvents, Sprunger *et al.*^{30,35-37} further modified the basic solvation model to include ion-specific equation coefficients:

$$\begin{aligned} \log P = & c_{p,\text{cation}} + c_{p,\text{anion}} + (e_{p,\text{cation}} + e_{p,\text{anion}}) \mathbf{E} \\ & + (s_{p,\text{cation}} + s_{p,\text{anion}}) \mathbf{S} + (a_{p,\text{cation}} + a_{p,\text{anion}}) \mathbf{A} \\ & + (b_{p,\text{cation}} + b_{p,\text{anion}}) \mathbf{B} + (v_{p,\text{cation}} + v_{p,\text{anion}}) \mathbf{V} \end{aligned} \quad (5)$$

$$\begin{aligned} \log K = & c_{k,\text{cation}} + c_{k,\text{anion}} + (e_{k,\text{cation}} + e_{k,\text{anion}}) \mathbf{E} \\ & + (s_{k,\text{cation}} + s_{k,\text{anion}}) \mathbf{S} + (a_{k,\text{cation}} + a_{k,\text{anion}}) \mathbf{A} \\ & + (b_{k,\text{cation}} + b_{k,\text{anion}}) \mathbf{B} + (l_{k,\text{cation}} + l_{k,\text{anion}}) \mathbf{L} \end{aligned} \quad (6)$$

Once calculated, the ion-specific equation coefficients can be summed to enable one to estimate solute partitioning behavior into a given IL as we will later illustrate. Thus far determined IL-specific equation coefficients have been determined for 30 different ILs (Eqns. 1 and 2), and 14 anion-specific coefficients and 21 cation-specific (Eqns. 5 and 6), based on experimentally measured infinite dilution activity coefficient data, gas chromatographic retention factors and solubilities of solutes dissolved in anhydrous IL solvents.¹⁹⁻³⁷ The fore-mentioned properties are thermodynamically related to the solute's Gibbs energies of transfer, gas-to-anhydrous IL and water-to-anhydrous IL partition coefficients. The water-to-anhydrous IL correlations describe "hypothetical" partitions, or more specifically a thermodynamic transfer process, in which the partition coefficient is calculated as the molar solubility ratio for the solute dissolved in both water and the anhydrous IL.

Each term on the right-hand side of Eqns. 1-6 represents a different type of solute-solvent interaction believed to be present in the solution. The interactions are determined by the polarity and hydrogen-bonding characteristics of the respective solute and solvent molecules. The uppercase variables (**E**, **S**, **A**, **B**, **V** and **L**) are solute-specific descriptors that have been determined for more than 5,000 different organic compounds and inorganic gases. The solute descriptors are defined as follows: **E** denotes the solute excess molar refraction in units of cm³ mol⁻¹/10 computed from the solute's refractive index; **S** corresponds to a combined dipolarity/polarizability descriptor; **A** and **B** describe the total hydrogen-bond acidity and basicity of the solute molecule, respectively; **V** is the McGowan characteristic molecular volume in units of cm³ mol⁻¹/100 and **L** is the logarithm of the gas-to-hexadecane partition coefficient measured at 298 K.

The set of six solvent/system coefficients in Eqns. 1-6 (*c_p*, *e_p*, *s_p*, *a_p*, *b_p*, *v_p*, *c_k*, *e_k*, *s_k*, *a_k*, *b_k* and *l_k*) characterize the given transfer process, and when multiplied by the respective solute descriptor quantify the strength of each type of solute-condensed phase interaction. Consequently, the equation coefficients are not merely adjustable curve-fitting parameters, but rather encode chemical knowledge concerning the properties of the specific condensed phase being described. These properties are defined as follows: *e* is a measure of the condensed phase interactions with the non-bonding and π-electrons of the solute molecule; *s* describes the dipolarity/polarizability of the condensed phase; *a* represents the condensed phase's hydrogen bond basicity (which is the complimentary property to solute's hydrogen bond acidity) and *b* is the condensed phase's hydrogen bond acidity (which is the complimentary property

to solute's hydrogen bond basicity). The *l* and *v* coefficients in Eqns. 1-6 reflect the general dispersion forces that facilitate solubility of a dissolved solute and the condensed phase-condensed phase interactions that oppose the solubilization process. In the case of solute transfer between water and an ionic liquid solvent (Eqns. 1, 3 and 5), the equation coefficients refer to differences in the properties of the aqueous and IL condensed phases.

In the present study, we report gas-liquid chromatographic retention factor data for a wide range of organic solutes on 1-methoxyethyl-1-methylpiperidinium *tris*(pentafluoroethyl)trifluorophosphate, ([MeoeMPip]⁺[FAP]⁻), stationary phases at 323 K and 353 K. See Figure 1 for the molecular structure of the ionic liquid solvent. Results of the chromatographic measurements, combined with published gas-to-liquid partition coefficient data for volatile solutes dissolved in ([MeoeMPip]⁺[FAP]⁻)³⁸ were used to derive Abraham model log *K* and log *P* correlations at 298 K and 323 K. We note that Marciniak and Wlazlo³⁸ previously reported on Abraham model correlations for ([MeoeMPip]⁺[FAP]⁻) at 318, 328, 338, 348, 358 and 368 K based on 62 experimental data points. The datasets used in deriving the published correlations did not include the more acidic phenolic and carboxylic acid solutes (solutes with large **A** values) and the lesser volatile organic compounds considered in the present study. As a result the expanse of predictive chemical space encompassed by the published Abraham model correlations is significantly less than that achieved by the correlations derived here. The predictive area of chemical space is important in that one should not use the derived equations to estimate log *P* and log *K* values for compounds whose solute descriptors fall outside of the range of solute descriptors used in obtaining the predictive equations. Several of the IL-specific Abraham model correlations that have been reported in the published literature were based on datasets containing only fairly volatile and nonacidic organic solutes. Correlation equations derived from such data sets do need to be updated as experimental data for more diverse chemical solutes become available.

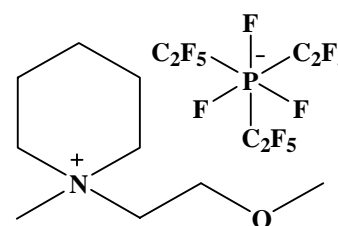


Figure 1. Molecular structure of 1-methoxy-ethyl-1-methylpiperidinium *tris*(pentafluoroethyl)trifluorophosphate.

2. Experimental Methods and Partition Coefficient Datasets

The sample of 1-methoxyethyl-1-methylpiperidinium *tris*(pentafluoroethyl)trifluorophosphate examined in this study was kindly donated as a gift from Merck KGaA (Darmstadt, Germany). The IL stationary phase was coated onto untreated fused silica capillary columns (5 m x 0.25 mm) obtained from Supelco (Bellefonte, PA). The IL coating solutions were prepared in dichloromethane using a 0.45% (w/v) concentration of [MeoeMPip]⁺[FAP]⁻.

Forty-four (44) probe molecules were selected for the characterization of the [MeoeMPip]⁺[FAP]⁻ stationary phase. The names of the solutes, along with the chemical suppliers and chemical purities, are given in Table 1. All solute molecules were used as received. The presence of trace impurities in these probes should in no way affect the results because the main chromatographic peak can be easily distinguished from any impurity peak by its much greater intensity.

Table 1. List of organic solutes, chemical suppliers, and chemical purities

Solute	Supplier ^a	Purity
Acetic acid	Supelco	99.7%
Acetophenone	Sigma-Aldrich	99%
Aniline	Sigma-Aldrich	99.5%
Benzaldehyde	Sigma-Aldrich	99+%
Benzene	Sigma-Aldrich	99.8%
Benzonitrile	Sigma-Aldrich	99%
Benzyl alcohol	Sigma-Aldrich	99%
1-Bromohexane	Sigma-Aldrich	98%
1-Bromooctane	Sigma-Aldrich	99%
Butyraldehyde	Acros Organics	99%
1-Butanol	Fisher Scientific	99.9%
2-Chloroaniline	Sigma-Aldrich	98%
1-Chlorobutane	Sigma-Aldrich	99%
1-Chlorohexane	Sigma-Aldrich	99%
1-Chlorooctane	Sigma-Aldrich	99%
<i>p</i> -Cresol	Fluka	99%
Cyclohexanol	J.T. Baker	99%
Cyclohexanone	Sigma-Aldrich	99.8%
1,2-Dichlorobenzene	Sigma-Aldrich	99%
1,4-Dioxane	Sigma-Aldrich	99.8%
N,N-Dimethylformamide	Fisher Scientific	99.9%
Ethyl acetate	Fisher Scientific	99.9%
Ethylbenzene	Eastman Kodak Co	95+%
1-Iodobutane	Sigma-Aldrich	99%
Methyl caproate	Supelco	98%
Naphthalene	Supelco	98%
Nitrobenzene	Sigma-Aldrich	99+%
2-Nitrophenol	Acros Organics	99%
1-Nitropropane	Sigma-Aldrich	99%
1-Octanol	Sigma-Aldrich	99+%
Octylaldehyde	Sigma-Aldrich	99%
1-Pentanol	Sigma-Aldrich	99+%
2-Pentanone	Sigma-Aldrich	99+%
Phenetole	Sigma-Aldrich	99%
Phenol	Sigma-Aldrich	99+%
Propionitrile	Sigma-Aldrich	99%
Pyridine	Sigma-Aldrich	99.9%
Toluene	Fisher Scientific	99.80%
<i>m</i> -Xylene	Fluka	99.5%
<i>o</i> -Xylene	Fluka	99.5%
<i>p</i> -Xylene	Fluka	99.5%
Propanoic acid	Supelco	99%
1-Decanol	Sigma-Aldrich	99+%
2-Propanol	Fisher Scientific	99.6%

^a Fluka (Steinheim, Germany); Eastman Kodak Company (Rochester, NY, USA); Supelco (Bellefonte, PA, USA); Acros Organics (Morris Plains, NJ, USA); J.T. Baker (Phillipsburg, NJ, USA); Sigma-Aldrich (St. Louis, MO, USA); and Fisher Scientific (Pittsburgh, PA, USA).

Chromatographic retention factors, k , were determined on a [MeoeMPip]⁺[FAP]⁻ stationary phase at 323 K and 353 K as part of the present study. The percent relative standard deviation (% RSD) in experimental retention times for all solutes included in this study was less than 1%. The stationary phase's integrity during the duration of the experimental measurements was established by periodically monitoring the retention factor and efficiency of naphthalene separation. The experimental $\log k$ values are tabulated in the second and third columns of Table 2. The extrapolated 298 K $\log k$ values obtained through a $\log k$ versus $1/T$ linear plot of the measured data at 323 K and 353 K are given in the table's last column.

The thermodynamic gas-to-IL partition coefficient, K , can be computed from isothermal chromatographic measurements through $K = V_N/V_L$, where V_N is the volume of the carrier gas required to elute the solute, and V_L is the volume of liquid present as the stationary phase.³⁹ The retention factor, k , is defined as³⁹ $k = (t_r - t_m)/t_m$ where t_r is the retention time of a solute and t_m is the "void" retention time for an unretained solute. Since $t_r - t_m$, the corrected retention time, is proportional to V_N , the corrected elution volume, it follows that gas-to-liquid partition coefficients and retention factors are interrelated,

$$K = P^* \cdot k \quad \text{or} \quad \log K = \log P^* + \log k \quad (7)$$

The proportionality constant, P^* , is the phase ratio and depends only upon the chromatographic conditions. The value of P^* should remain essentially constant for a given column during the time the experimental measurements are performed.

Thermodynamic gas-to-IL partition coefficients are required to calculate the proportionality constants needed in Eqn. 8 for converting the measured $\log k$ data in Table 2 to $\log K$ values. Marciniak and Wlazlo³⁸ reported infinite dilution activity coefficients and gas-to-liquid partition coefficients of 62 solutes dissolved in [MeoeMPip]⁺[FAP]⁻ in the 318 to 368 K temperature range. Uncertainties in the measured K and $\gamma_{\text{solute}}^\infty$ values were reported to be on the order of 2 to 3%. The published experimental data were extrapolated to 298 K and 323 K by assuming a linear $\ln K$ versus $1/T$ relationship. A linear extrapolation should be valid as the measurements were performed not too far removed from the desired temperatures (less than 20 K in most instances). The $\log P$ values for partition from water to the anhydrous IL can be calculated via Eqn. 8

$$\log P = \log K - \log K_w \quad (8)$$

The conversion of $\log K$ data to $\log P$ requires a prior knowledge of the solute's gas phase partition coefficient into water, K_w , which is available for most of the solutes being studied. As noted above, water-to-anhydrous IL partition coefficients (more formally called Gibbs energy of solute transfer when multiplied by $-2.303 RT$) calculated through Eqn. 8 refer to a hypothetical partitioning process involving solute transfer from water to the anhydrous IL. $\log P$ values calculated in this fashion are still useful because the predicted $\log P$ values can be used to estimate the solute's infinite dilution activity coefficient in the IL.

The proportionality constants needed in Eqn. 7; $\log P^* = 2.555$ (298 K) and $\log P^* = 2.498$ (323 K) for [MeoeMPip]⁺[FAP]⁻ were the calculated average differences between the measured $\log k$ and $\log K$ values for

Table 2. Chromatographic retention factor data for organic solutes on 1-methoxyethyl-1-methylpiperidinium tris(pentafluoroethyl)-trifluorophosphate, ([MeoeMPip]⁺[FAP]⁻), stationary phase at 298, 323, and 353 K

Solute	log k (323 K)	log k (353 K)	log k (298 K)
Acetic acid	0.446	-0.096	0.981
Acetophenone	2.172	1.466	2.869
Aniline	2.187	1.462	2.902
Benzaldehyde	1.662	1.027	2.289
Benzene	0.037	-0.405	0.474
Benzonitrile	1.810	1.177	2.435
Benzyl alcohol	2.150	1.421	2.870
1-Bromooctane	0.983	0.370	1.589
1-Butanol	0.143	-0.341	0.622
Butyraldehyde	0.087	-0.352	0.520
2-Chloroaniline	2.284	1.558	3.001
1-Chlorobutane	-0.495		
1-Chlorohexane	0.129	-0.354	0.606
1-Chlorooctane	0.736	0.155	1.309
<i>p</i> -Cresol	2.173	1.420	2.915
Cyclohexanol	0.922	0.343	1.493
Cyclohexanone	1.384	0.804	1.957
1,2-Dichlorobenzene	1.111	0.540	1.675
N,N-Dimethylformamide	1.925	1.288	2.554
1,4-Dioxane	0.578	0.059	1.090
Ethyl acetate	0.142	-0.334	0.610
Ethylbenzene	0.649	0.105	1.186
1-Iodobutane	-0.028	-0.452	0.392
Methyl Caproate	1.019	0.404	1.626
Naphthalene	2.288	1.580	2.988
Nitrobenzene	2.040	1.379	2.693
1-Nitropropane	0.939	0.409	1.461
1-Octanol	1.372	0.690	2.045
Octylaldehyde	1.305	0.667	1.935
1-Pentanol	0.462	-0.065	0.981
2-Pentanone	0.587	0.080	1.087
Phenetole	1.394	0.756	2.023
Phenol	1.855	1.161	2.539
Propionitrile	0.537	0.082	0.986
Pyridine	0.813	0.300	1.320
Pyrrole	1.329	0.722	1.929
Toluene	0.388	-0.103	0.873
<i>m</i> -Xylene	0.731	0.179	1.276
<i>o</i> -Xylene	0.836	0.277	1.387
<i>p</i> -Xylene	0.705	0.154	1.248
2-Propanol	-0.385		
2-Nitrophenol	1.960	1.291	2.621
1-Bromohexane	0.364	-0.128	0.849
Propanoic acid	0.731	0.133	1.321
1-Decanol	1.970	1.188	2.742

the 12 common compounds (i.e., benzene, 1-butanol, butyraldehyde, ethyl acetate, ethylbenzene, 1-nitropropane, 2-pentanone, pyridine, toluene, *m*-xylene, *o*-xylene and *p*-xylene) in the IL's data set that had been studied by us and by Marciniak and Wlazlo.³⁸ The calculated $\log K$ and $\log P$ values are compiled in Table 3 for solutes dissolved in [MeoeMPip]⁺[FAP]⁻. $\log P$ values are tabulated only for

298 K as we do not have experimental values for the solutes' gas-to-water partition coefficients, $\log K_w$, at 323 K. The $\log K_w$ values that we have compiled to date pertain to gas to water partitioning at 298 K⁴⁰ and 310 K,⁴¹ or for gas to physiological saline partitioning at 310 K.⁴¹ For the convenience of the reader, we have compiled the numerical values of solute descriptors for the 90 organic compounds considered in the present study in Table 4. The solute descriptors are of experimental origin, and were retrieved from the Abraham database. The numerical values were deduced from experimental solubility data, gas-liquid and high-performance liquid chromatographic retention factor measurements and water-to-solvent partition determinations as discussed by Abraham and coworkers⁴²⁻⁴⁴ in several published papers.

3. Results and Discussion

We have tabulated in Table 3 the experimental $\log K$ values and $\log P$ values for a chemically diverse set of 90 organic compounds in [MeoeMPip]⁺[FAP]⁻. The solutes span a large range of molecular size and shape, polarity and hydrogen-bonding characteristics. Preliminary analysis of the experimental data in Table 3 in accordance with Eqns. 1 and 2 of the Abraham general solvation parameter model revealed that the e_k equation coefficient ($e_k = 0.008 \pm 0.092$ and 0.040 ± 0.069) was negligible in both the $\log K$ (298 K) and $\log K$ (323 K) correlation. The $e_k \mathbf{E}$ term was consequently removed from the 298 K and 323 K $\log K$ correlations, and the regression analyses were rerun to yield the following three LFERs:

$$\begin{aligned} \log K (298 \text{ K}) = & -0.177 (0.061) + 2.311(0.056) \mathbf{S} \\ & + 1.249(0.091) \mathbf{A} + 0.542(0.090) \mathbf{B} \\ & + 0.655(0.017) \mathbf{L} \end{aligned} \quad (8)$$

(N = 103, SD = 0.137, R² = 0.984, F = 1534)

$$\begin{aligned} \log K (323 \text{ K}) = & -0.298(0.050) + 2.126(0.047) \mathbf{S} \\ & + 1.056(0.076) \mathbf{A} + 0.447(0.075) \mathbf{B} \\ & + 0.567(0.014) \mathbf{L} \end{aligned} \quad (9)$$

(N = 105, SD = 0.116, R² = 0.986, F = 1747)

$$\begin{aligned} \log P (298 \text{ K}) = & 0.114(0.091) + 0.260(0.091) \mathbf{E} \\ & + 0.391(0.103) \mathbf{S} - 2.448(0.114) \mathbf{A} \\ & - 4.245(0.128) \mathbf{B} + 3.281(0.079) \mathbf{V} \end{aligned} \quad (10)$$

(N = 103, SD = 0.163, R² = 0.989, F = 1755)

where the standard errors in the calculated equation coefficients are given in parentheses. The statistical information associated with each correlation includes the number of experimental data points (N), the standard deviation (SD), the squared correlation coefficient (R²) and the Fisher F-statistic (F). The number of data points used in the regression analyses is larger than the number of solutes studied because the thirteen solutes needed in the $\log P^*$ computation appear twice – first in top thermodynamic dataset and then later in the chromatographic retention factor dataset.

Table 3. Logarithm of the gas-to-anhydrous IL partition coefficient, log *K*, and logarithm of the water-to-anhydrous IL partition coefficient, log *P*, for organic solutes dissolved in [MeoeMPip]⁺[FAP]⁻ at 298 K and 323 K

Solute	log <i>K</i> (298 K)	log <i>K</i> (323 K)	log <i>P</i> (298 K)
<i>Based on Thermodynamic Data</i>			
Pentane	1.118	0.832	2.818
Hexane	1.488	1.142	3.308
3-Methylpentane	1.449	1.120	3.289
2,2-Dimethylbutane	1.274	0.978	3.114
Heptane	1.844	1.450	3.804
Octane	2.198	1.753	4.308
2,2,4-Trimethylpentane	1.859	1.476	3.979
Nonane	2.559	2.055	4.709
Decane	2.914	2.355	5.234
Cyclopentane	1.508	1.194	2.388
Cyclohexane	1.837	1.486	2.737
Methylcyclohexane	2.051	1.661	3.301
Cycloheptane	2.349	1.925	2.929
Cyclooctane	2.784	2.309	3.554
1-Pentene	1.354	1.042	2.584
1-Hexene	1.727	1.357	2.887
Cyclohexene	2.151	1.752	2.421
1-Heptene	2.084	1.660	3.304
1-Octene	2.445	1.963	3.855
1-Decene	3.122	2.551	4.762
1-Pentyne	1.885	1.504	1.895
1-Hexyne	2.242	1.809	2.542
1-Heptyne	2.606	2.115	3.046
1-Octyne	2.943	2.412	3.463
Benzene	3.036	2.547	2.406
Toluene	3.432	2.888	2.782
Ethylbenzene	3.736	3.148	3.156
<i>o</i> -Xylene	3.947	3.337	3.287
<i>m</i> -Xylene	3.840	3.235	3.230
<i>p</i> -Xylene	3.804	3.201	3.214
Styrene	4.142	3.508	3.192
α -Methylstyrene	4.361	3.684	3.401
Methanol	2.197	1.808	-1.543
Ethanol	2.436	2.006	-1.234
1-Propanol	2.790	2.303	-0.770
2-Propanol	2.563	2.101	-0.917
1-Butanol	3.192	2.636	-0.268
2-Butanol	2.915	2.392	-0.475
2-Methyl-1-propanol	2.986	2.473	-0.314
<i>tert</i> -Butanol	2.673	2.177	-0.607
Thiophene	3.083	2.593	2.043
Tetrahydrofuran	2.917	2.447	0.367
1,4-Dioxane	3.643	3.078	-0.067
Methyl <i>tert</i> -butyl ether	2.244	1.817	0.624
Ethyl <i>tert</i> -butyl ether	2.151	1.722	0.881
Methyl <i>tert</i> -amyl ether	2.589	2.115	1.119
Diethyl ether	1.900	1.514	0.730
Dipropyl ether	2.408	1.947	1.518
Diisopropyl ether	2.091	1.663	1.041
Dibutyl ether	3.063	2.509	2.373
Acetone	3.037	2.572	0.247
2-Pentanone	3.644	3.089	1.064

Table 3. (cont.)

Solute	log <i>K</i> (298 K)	log <i>K</i> (323 K)	log <i>P</i> (298 K)
<i>Based on Thermodynamic Data</i>			
3-Pentanone	3.639	3.080	1.139
Methyl acetate	2.886	2.414	0.586
Ethyl acetate	3.154	2.639	0.994
Methyl propanoate	3.203	2.678	1.053
Methyl butanoate	3.491	2.927	1.411
Butyraldehyde	3.067	2.585	0.737
Acetonitrile	3.314	2.849	0.464
Pyridine	3.857	3.284	0.417
1-Nitropropane	4.021	3.446	1.571
<i>Based on Chromatographic Retention Factor Data</i>			
Acetic acid	3.536	2.944	-1.374
Acetophenone	5.424	4.670	2.154
Aniline	5.457	4.685	1.375
Benzaldehyde	4.844	4.160	1.894
Benzene	3.029	2.535	2.399
Benzonitrile	4.990	4.308	1.900
Benzyl alcohol	5.425	4.648	0.565
1-Bromooctane	4.144	3.481	4.524
Butyraldehyde	3.075	2.585	0.745
1-Butanol	3.177	2.641	-0.283
2-Chloroaniline	5.556	4.782	1.956
1-Chlorobutane		2.003	
1-Chlorohexane	3.161	2.627	3.161
1-Chlorooctane	3.864	3.234	4.054
<i>p</i> -Cresol	5.470	4.671	0.970
Cyclohexanol	4.048	3.420	0.038
Cyclohexanone	4.512	3.882	0.912
1,2-Dichlorobenzene	4.230	3.609	3.330
1,4-Dioxane	3.645	3.076	-0.065
<i>N,N</i> -Dimethylformamide	5.109	4.423	-0.621
Ethyl acetate	3.165	2.640	1.005
Ethyl benzene	3.741	3.147	3.161
1-Iodobutane	2.947	2.470	2.767
Methyl caproate	4.181	3.517	2.351
Naphthalene	5.543	4.786	3.813
Nitrobenzene	5.248	4.538	2.228
2-Nitrophenol	5.176	4.458	1.816
1-Nitropropane	4.016	3.437	1.566
1-Octanol	4.600	3.870	1.600
Octylaldehyde	4.490	3.803	2.810
1-Pentanol	3.536	2.960	0.186
2-Pentanone	3.642	3.085	1.062
Phenetole	4.578	3.892	2.948
Phenol	5.094	4.353	0.244
2-Propanol		2.113	
Propionitrile	3.541	3.035	0.721
Pyridine	3.875	3.311	0.435
Toluene	3.428	2.886	2.778
<i>m</i> -Xylene	3.831	3.229	3.221
<i>o</i> -Xylene	3.942	3.334	3.282
<i>p</i> -Xylene	3.803	3.203	3.213
1-Bromohexane	3.404	2.862	3.534
Propanoic acid	3.876	3.229	-0.864
1-Decanol	5.297	4.468	2.627

Table 4. Abraham model solute descriptors of the organic compounds considered in the present study

Solute	E	S	A	B	L	V
Pentane	0.000	0.000	0.000	0.000	2.162	0.8131
Hexane	0.000	0.000	0.000	0.000	2.668	0.9540
3-Methylpentane	0.000	0.000	0.000	0.000	2.581	0.9540
2,2-Dimethylbutane	0.000	0.000	0.000	0.000	2.352	0.9540
Heptane	0.000	0.000	0.000	0.000	3.173	1.0949
Octane	0.000	0.000	0.000	0.000	3.677	1.2358
2,2,4-Trimethylpentane	0.000	0.000	0.000	0.000	3.106	1.2358
Nonane	0.000	0.000	0.000	0.000	4.182	1.3767
Decane	0.000	0.000	0.000	0.000	4.686	1.5176
Cyclopentane	0.263	0.100	0.000	0.000	2.477	0.7045
Cyclohexane	0.305	0.100	0.000	0.000	2.964	0.8454
Methylcyclohexane	0.244	0.060	0.000	0.000	3.319	0.9863
Cycloheptane	0.350	0.100	0.000	0.000	3.704	0.9863
Cyclooctane	0.413	0.100	0.000	0.000	4.329	1.1272
1-Pentene	0.093	0.080	0.000	0.070	2.047	0.7701
1-Hexene	0.078	0.080	0.000	0.070	2.572	0.9110
Cyclohexene	0.395	0.280	0.000	0.090	2.952	0.8204
1-Heptene	0.092	0.080	0.000	0.070	3.063	1.0519
1-Octene	0.094	0.080	0.000	0.070	3.568	1.1928
1-Decene	0.093	0.080	0.000	0.070	4.554	1.4746
1-Pentyne	0.172	0.230	0.120	0.120	2.010	0.7271
1-Hexyne	0.166	0.220	0.100	0.120	2.510	0.8680
1-Heptyne	0.160	0.230	0.120	0.100	3.000	1.0089
1-Octyne	0.155	0.220	0.090	0.100	3.521	1.1498
Benzene	0.610	0.520	0.000	0.140	2.786	0.7164
Toluene	0.601	0.520	0.000	0.140	3.325	0.8573
Ethylbenzene	0.613	0.510	0.000	0.150	3.778	0.9982
<i>o</i> -Xylene	0.663	0.560	0.000	0.160	3.939	0.9982
<i>m</i> -Xylene	0.623	0.520	0.000	0.160	3.839	0.9982
<i>p</i> -Xylene	0.613	0.520	0.000	0.160	3.839	0.9982
Styrene	0.849	0.650	0.000	0.160	3.908	0.9550
α -Methylstyrene	0.851	0.640	0.000	0.190	4.290	1.0960
Methanol	0.278	0.440	0.430	0.470	0.970	0.3082
Ethanol	0.246	0.420	0.370	0.480	1.485	0.4491
1-Propanol	0.236	0.420	0.370	0.480	2.031	0.5900
2-Propanol	0.212	0.360	0.330	0.560	1.764	0.5900
1-Butanol	0.224	0.420	0.370	0.480	2.601	0.7310
2-Butanol	0.217	0.360	0.330	0.560	2.338	0.7310
2-Methyl-1-propanol	0.217	0.390	0.370	0.480	2.413	0.7310
<i>tert</i> -Butanol	0.180	0.300	0.310	0.600	1.963	0.7310
Thiophene	0.687	0.570	0.000	0.150	2.819	0.6411
Tetrahydrofuran	0.289	0.520	0.000	0.480	2.636	0.6223
1,4-Dioxane	0.329	0.750	0.000	0.640	2.892	0.6810
Methyl <i>tert</i> -butyl ether	0.024	0.220	0.000	0.550	2.372	0.8718
Ethyl <i>tert</i> -butyl ether	-0.020	0.160	0.000	0.600	2.720	1.0127
Methyl <i>tert</i> -amyl ether	0.050	0.210	0.000	0.600	2.916	1.0127
Diethyl ether	0.041	0.250	0.000	0.450	2.015	0.7309
Dipropyl ether	0.008	0.250	0.000	0.450	2.954	1.0127
Diisopropyl ether	-0.063	0.170	0.000	0.570	2.501	1.0127
Dibutyl ether	0.000	0.250	0.000	0.450	3.924	1.2945
Acetone	0.179	0.700	0.040	0.490	1.696	0.5470
2-Pentanone	0.143	0.680	0.000	0.510	2.755	0.8288
3-Pentanone	0.154	0.660	0.000	0.510	2.811	0.8288
Methyl acetate	0.142	0.640	0.000	0.450	1.911	0.6057
Ethyl acetate	0.106	0.620	0.000	0.450	2.314	0.7466
Methyl propanoate	0.128	0.600	0.000	0.450	2.431	0.7470
Methyl butanoate	0.106	0.600	0.000	0.450	2.943	0.8880
Butyraldehyde	0.187	0.650	0.000	0.450	2.270	0.6880
Acetonitrile	0.237	0.900	0.070	0.320	1.739	0.4040
Pyridine	0.631	0.840	0.000	0.520	3.022	0.6753

Table 4. (cont.)

Solute	E	S	A	B	L	V
1-Nitropropane	0.242	0.950	0.000	0.310	2.894	0.7055
Acetic acid	0.265	0.640	0.620	0.440	1.816	0.4648
Acetophenone	0.818	1.010	0.000	0.480	4.501	1.0139
Aniline	0.955	0.960	0.260	0.410	3.934	0.8162
Benzaldehyde	0.820	1.000	0.000	0.390	4.008	0.8730
Benzonitrile	0.742	1.110	0.000	0.330	4.039	0.8711
Benzyl alcohol	0.803	0.870	0.330	0.560	4.221	0.9160
1-Bromooctane	0.339	0.400	0.000	0.120	5.143	1.4108
2-Chloroaniline	1.033	0.920	0.250	0.310	4.674	0.9390
1-Chlorobutane	0.210	0.400	0.000	0.100	2.722	0.7946
1-Chlorohexane	0.201	0.390	0.000	0.090	3.708	1.0764
1-Chlorooctane	0.191	0.400	0.000	0.090	4.708	1.3582
<i>p</i> -Cresol	0.820	0.870	0.570	0.310	4.312	0.9160
Cyclohexanol	0.460	0.540	0.320	0.570	3.758	0.9040
Cyclohexanone	0.403	0.860	0.000	0.560	3.792	0.8611
1,2-Dichlorobenzene	0.872	0.780	0.000	0.040	4.318	0.9612
N,N-Dimethylformamide	0.367	1.310	0.000	0.740	3.173	0.6468
1-Iodobutane	0.628	0.400	0.000	0.150	3.628	0.9304
Methyl caproate	0.080	0.600	0.000	0.450	3.874	1.1693
Naphthalene	1.340	0.920	0.000	0.200	5.161	1.0854
Nitrobenzene	0.871	1.110	0.000	0.280	4.557	0.8906
2-Nitrophenol	1.015	1.050	0.050	0.370	4.760	0.9493
1-Octanol	0.199	0.420	0.370	0.480	4.619	1.2950
Octylaldehyde	0.160	0.650	0.000	0.450	4.380	1.2515
1-Pentanol	0.219	0.420	0.370	0.480	3.106	0.8718
2-Pentanone	0.143	0.680	0.000	0.510	2.755	0.8288
Phenetole	0.681	0.700	0.000	0.320	4.242	1.0569
Phenol	0.805	0.890	0.600	0.300	3.766	0.7751
Propionitrile	0.162	0.900	0.020	0.360	2.082	0.5450
1-Bromohexane	0.349	0.400	0.000	0.120	4.130	1.1290
Propionic acid	0.233	0.650	0.600	0.450	2.290	0.6057
1-Decanol	0.191	0.420	0.370	0.480	5.610	1.5763

All regression analyses were performed using SPSS Statistics (Version 20) software. The LFERs described by Eqns. 8 – 10 are statistically quite good with standard deviations of less than 0.165 log units. Figure 2 shows a plot of log *K* (298) values predicted from Eqn. 8 against experimental values covering a range of approximately 4.44 log units, from log *K* = 1.118 for pentane to log *K* = 5.556 for 2-chloronaphthalene. A comparison of the calculated versus experimental log *P* data is shown in Figure 2. As expected the standard deviation for the log *P* correlation is slightly larger than that of the log *K* correlations because the log *P* values contain the additional experimental uncertainty in the gas-to-water used in the log *K* to log *P* conversion.

The equation coefficients in Eqn. 9 can be compared to those reported by Marciniak and Wlazlo.³⁸ As noted above the authors determined log *K* correlations based on experimental gas-to-liquid partition coefficient data for 55 different compounds measured at temperatures of 318, 328, 338, 348, 358 and 368 K. While 323 K was not one of the temperatures studied by the authors, one should be able to reasonably assume that a log *K* correlation for 323 K should fall somewhere between the reported correlations

$$\begin{aligned} \log K (318 \text{ K}) = & -0.386(0.067) - 0.004(0.082) \mathbf{E} \\ & + 2.35(0.08) \mathbf{S} + 1.17(0.12) \mathbf{A} \\ & + 0.391(0.084) \mathbf{B} + 0.607(0.020) \mathbf{L} \end{aligned} \quad (11)$$

$$\begin{aligned} \log K (328 \text{ K}) = & -0.409(0.062) + 0.005(0.076) \mathbf{E} \\ & + 2.26(0.08) \mathbf{S} + 1.09(0.12) \mathbf{A} \\ & + 0.354(0.079) \mathbf{B} + 0.569(0.019) \mathbf{L} \end{aligned} \quad (12)$$

for 318 K and 328 K. Comparison of Eqns. 9, 11 and 12 shows that our calculated equation coefficients for the 323 log *K* correlation do fall in between those reported for the Marciniak and Wlazlo for 318 K and 328 K when the combined standard errors in the coefficients are taken into account. The slight difference between our coefficients and the arithmetic average of the coefficients of Eqns. 11 and 12 likely results from the more diverse set of solutes used in deriving Eqn. 9. Our dataset (see Table 3) has 105 data points and includes two carboxylic acid solutes (acetic acid and propanoic acid), two primary amine solutes (aniline and 2-chloroaniline), three phenolic compounds (phenol, 2-nitrophenol and *p*-cresol), several substituted aromatic benzene derivatives (nitrobenzene, benzonitrile, acetophenone, benzaldehyde, phenetole, 1,2-dichlorobenzene, benzyl alcohol), and

several halogenated alkanes (1-chlorobutane, 1-chlorohexane, 1-chlorooctane, 1-iodobutane, 1-bromohexane, 1-bromooctane) plus the solutes (and data) from the Marciniak and Wlazlo study.³⁸ We also note that Marciniak and Wlazlo did not report a log *K* correlation for 298 K, nor did the authors correlate the water-to-anhydrous ionic liquid transfer properties.

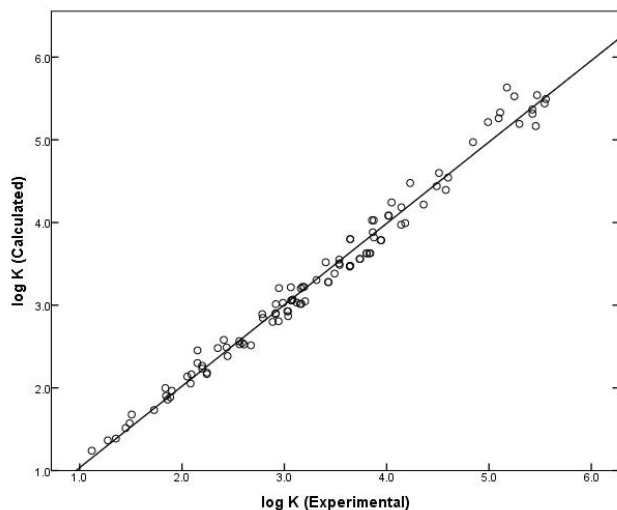


Figure 2. Comparison between experimental log *K* (298 K) data and predicted values based on Eqn. 8

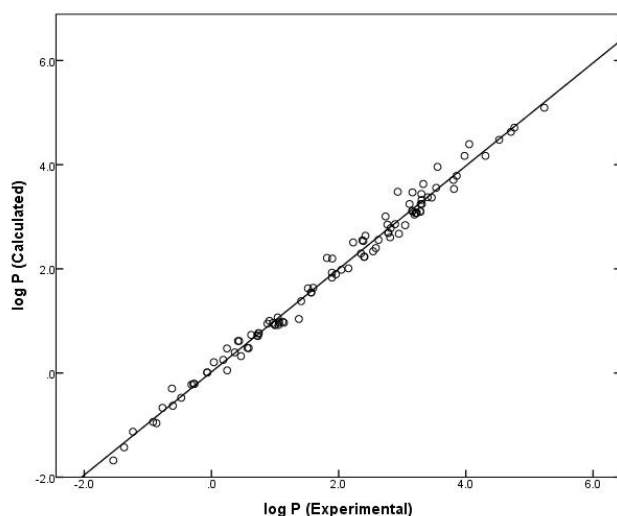


Figure 3. Comparison between experimental log *P* (298 K) data and predicted values based on Eqn. 10

One small change that has made in the present study concerns converting the measured log *K* value to log *P*. We are using a value of log *K_w* = -0.77 for the logarithm of the gas-to-water partition coefficient of cyclooctane45 in the log *K* to log *P* conversions, which is a departure from several earlier studies. Stephens et al.³¹ observed that the value of log *K_w* = -0.77 for cyclooctane led to slightly smaller standard deviations in the log *P* correlations of 1-butyl-1-methylpyrrolidinium tetracyanoborate and 1-butyl-1-methylpiperidinium bis(trifluoromethylsulfonyl)imide. The standard deviations in the derived correlations are slightly larger than the uncertainty in the measured data, which we estimate to be

on the order of approximately ± 0.07 to 0.10 log units. Our estimated uncertainty includes not only the uncertainties in the measured *K* data, but also the uncertainties involved in extrapolating the measured values to 298 K and in the calculated proportionality constant, *P*^{*}, needed to convert the chromatographic retention factors to gas-to-liquid partition coefficients.

Equations 8 – 10 can be utilized to estimate the infinite dilution activity coefficients and chromatographic retention factors of solutes dissolved in anhydrous [MeoeMPip]⁺[FAP]⁻. The predicted log *K* and log *P* values could be easily converted to $\gamma_{\text{solute}}^{\infty}$ values through Eqns. 13 and 14

$$\log K = \log \left(\frac{RT}{\gamma_{\text{solute}}^{\infty} P_{\text{solute}}^{\circ} V_{\text{solvent}}} \right) \quad (13)$$

$$\log P + \log K_w = \log \left(\frac{RT}{\gamma_{\text{solute}}^{\infty} P_{\text{solute}}^{\circ} V_{\text{solvent}}} \right) \quad (14)$$

where $P_{\text{solute}}^{\circ}$ is the vapor pressure of the solute at the system temperature (*T*), V_{solvent} is the molar volume of the IL solvent, and *R* is the universal gas constant. Infinite dilution activity coefficients play an important role in chemical separations in that the ratio of $\gamma_{\text{solute}}^{\infty}$ values for two solutes is called the selectivity factor which measures the enhanced separation that one could get from solute interactions with the ionic liquid phase solvent. In the case of chromatographic retention factors, one will need to measure log *k* values for a few standard “calibration” solutes using the actual coated chromatographic column in order to obtain the phase ratio (*P*^{*} in Eqn. 7) needed to convert the predicted log *K* values to log *k* values.

In order to assess properly the predictive capabilities and limitations of Eqns. 8–10, we divided each of the three large data sets into training sets and test sets by allowing the SPSS software to randomly select half of the experimental data points. The selected data points became the training sets and the compounds that were left served as the test sets. Analysis of the experimental data in the two log *K* and single log *P* training sets gave

$$\begin{aligned} \log K (298) = & -0.120(0.088) + 2.260(0.076) \mathbf{S} \\ & + 1.242(0.107) \mathbf{A} + 0.556(0.123) \mathbf{B} \\ & + 0.644 (0.023) \mathbf{L} \end{aligned} \quad (15)$$

(*N* = 52, *SD* = 0.137, *R*² = 0.984, *F* = 704)

$$\begin{aligned} \log K (323) = & -0.326(0.073) + 2.115(0.078) \mathbf{S} \\ & + 1.179(0.169) \mathbf{A} + 0.425(0.128) \mathbf{B} \\ & + 0.574(0.021) \mathbf{L} \end{aligned} \quad (16)$$

(*N* = 53, *SD* = 0.119, *R*² = 0.985, *F* = 765)

$$\begin{aligned} \log P (298) = & 0.075(0.128) + 0.129(0.121) \mathbf{E} \\ & + 0.515(0.144) \mathbf{S} - 2.490(0.141) \mathbf{A} \\ & - 4.211(0.171) \mathbf{B} + 3.315(0.110) \mathbf{V} \end{aligned} \quad (17)$$

(*N* = 52, *SD* = 0.160, *R*² = 0.989, *F* = 852)

Careful examination of Eqns. 8 – 10 and Eqns. 15 – 17 reveals that to within the standard errors in the equation coefficients, the training set equation coefficients are identical to the equation coefficients for the full data sets. The training set expressions were then used to estimate the gas-to-IL partition coefficients for the 51 compounds in the log *K* test sets, and the water-to-IL partition coefficients of the 51 compounds in the log *P* test set. For the estimated and experimental values we found SD values of 0.142, 0.116 and 0.174; average absolute error (AAE) values of 0.122, 0.097 and 0.143; and average error (AE) values of 0.004, 0.012 and -0.028 for Eqns. 15–17, respectively. The small AE values indicate that there was very little bias in generating these estimated log *K* and log *P* values. The training and test set analyses were performed two more times with very similar statistical results.

The derived Abraham model correlations are expected to provide reasonably accurate partition coefficient predictions for additional organic compounds in anhydrous [MeoeMPip]⁺[FAP]⁻ provided that solute's descriptor values fall within the range of **E** = 0.000 to 1.340; **S** = 0.000 to 1.310; **A** = 0.000 to 0.620; **B** = 0.000 to 0.740; **V** = 0.308 to 1.576; and **L** = 0.970 to 5.610. As an informational note, small gaseous solutes like carbon dioxide, methane, ethene, *etc.* would not be included in the above descriptor range because their **V** and **L** solute descriptors are too small. We were not able to find gas solubility data for these small solutes dissolved in anhydrous [MeoeMPip]⁺[FAP]⁻.

For ionic liquid solvents, Sprunger *et al.*^{35,36} assumed that each equation coefficient could be separated into a cationic and an anionic contribution according to Eqns. 5 and 6 above. The authors proposed a relatively simple computation methodology for obtaining ion-specific equation coefficients for additional cations/anions based on previously calculated ion-specific equation coefficients. [FAP]⁻-specific equation coefficients of $c_{k,anion} = 0.179$; $e_{k,anion} = -0.015$; $s_{k,anion} = 0.063$; $a_{k,anion} = -1.314$; $b_{k,anion} = 0.238$ and $l_{k,anion} = -0.053$ ³² have been previously reported. The above [FAP]⁻-specific equation coefficients pertain to the log *K* Abraham model correlation for 298 K. The equation coefficients for the [MeoeMPip]⁺ are computed by subtracting the existing [FAP]⁻-specific equation coefficients from the values given in Eqn. 8. Performing the indicated computation, the following numerical values of $c_{k,cation} = -0.356$; $e_{k,cation} = 0.015$; $s_{k,cation} = 2.248$; $a_{k,cation} = 2.563$; $b_{k,cation} = 0.304$ and $l_{k,cation} = 0.708$ are obtained for the [MeoeMPip]⁺ cation. Numerical values for the [MeoeMPip]⁺ cation for the log *P* (298 K) correlation would be calculated in similar using published values³² of $c_{p,anion} = 0.132$; $e_{p,anion} = -0.171$; $s_{p,anion} = 0.121$; $a_{p,anion} = -1.314$; $b_{p,anion} = 0.244$ and $v_{p,anion} = -0.107$ for the [FAP]⁻ anion in conjunction with Eqn. 10.

The calculated [FAP]⁻-specific equation coefficients can be combined with existing known values for other anions to generate Abraham model correlations for predicting gas-to-liquid partition coefficients of solutes dissolved in other anhydrous ionic liquid. For example, the Abraham model correlation for predicting gas-to-liquid partition coefficients of solutes in 1-methoxyethyl-

Table 5. Comparison of Experimental log *K* (298) Data and Predicted Values Based on Eqn. 18

Solute	log <i>K</i> _{exp}	log <i>K</i> _{pred}
Pentane	0.965	1.175
Hexane	1.318	1.533
3-Methylpentane	1.295	1.471
2,2-Dimethylbutane	1.113	1.309
Heptane	1.663	1.890
Octane	1.998	2.247
2,2,4-Trimethylpentane	1.650	1.843
Nonane	2.338	2.605
Decane	2.669	2.962
Cyclopentane	1.414	1.626
Cyclohexane	1.752	1.972
Methylcyclohexane	1.927	2.132
Cycloheptane	2.248	2.496
Cyclooctane	2.689	2.940
1-Pentene	1.190	1.296
1-Hexene	1.536	1.667
Cyclohexene	2.058	2.397
1-Heptene	1.889	2.015
1-Octene	2.227	2.373
1-Decene	2.888	3.071
1-Hexyne	2.187	2.211
1-Heptyne	2.527	2.625
1-Octyne	2.863	2.895
Benzene	2.850	2.837
Toluene	3.225	3.219
Ethylbenzene	3.515	3.520
<i>o</i> -Xylene	3.739	3.750
<i>m</i> -Xylene	3.604	3.589
<i>p</i> -Xylene	3.587	3.589
Styrene	3.970	3.933
α -Methylstyrene	4.179	4.191
Methanol	2.469	2.569
Ethanol	2.677	2.737
1-Propanol	3.026	3.124
2-Propanol	2.761	2.721
1-Butanol	3.403	3.527
2-Butanol	3.083	3.128
2-Methyl-1-propanol	3.222	3.327
Thiophene	2.997	2.977
Tetrahydrofuran	2.709	2.830
1,4-Dioxane	3.440	3.577
Methyl <i>tert</i> -butyl ether	1.995	1.985
Ethyl <i>tert</i> -butyl ether	1.897	2.139
Methyl <i>tert</i> -amyl ether	2.328	2.364
Diethyl ether	1.639	1.770
Dipropyl ether	2.150	2.434
Diisopropyl ether	1.809	1.969
Dibutyl ether	2.781	3.121
Acetone	2.779	2.673
2-Pentanone	3.349	3.280
3-Pentanone	3.334	3.275
Methyl acetate	2.627	2.575
Ethyl Acetate	2.864	2.814
Methyl propanoate	2.917	2.853
Methyl butanoate	3.191	3.215
Butanal	2.855	2.852
Acetonitrile	3.163	3.179
Pyridine	3.731	3.839
1-Nitropropane	3.913	3.926

1-methylpiperidinium bis(trifluoro-methylsulfonyl)imide, [MeoeMPip]⁺[(Tf)₂N]⁻, is simply

$$\log K (298) = -0.356 + 0.015 E + 2.248 S + 2.563 A + 0.304 B + 0.708 L \quad (18)$$

as the [(Tf)₂N]⁻-specific equation coefficients are $c_{k,\text{anion}} = 0.000$; $e_{k,\text{anion}} = 0.000$; $s_{k,\text{anion}} = 0.000$; $a_{k,\text{anion}} = 0.000$; $b_{k,\text{anion}} = 0.000$ and $l_{k,\text{anion}} = 0.000$.^{35,36} In establishing the computation methodology, equation coefficients for the bis(trifluoromethylsulfonyl)imide anion were set equal to zero to provide a reference point from which all other equation coefficients would be calculated. The cation- and anion-specific equation coefficients appear in the Abraham model as a summed pair, and one needs a reference point for isolating an unique set of individual cation and anion values. In many respects this is analogous to setting a reference point for calculating thermodynamic properties of single ions.

The predictive ability of Eqn. 18 can be assessed using the recently published experimental data of Marciniak and Wlazlo⁴⁶ for 60 organic solutes dissolved in [MeoeMPip]⁺[(Tf)₂N]⁻ at temperatures from 318.15 to 368.15 K. The measured log *K* (298 K) needed for comparison against the predicted values based on Eqn. 18 were obtained by extrapolating the 318.15 K and 328.15 K log *K* data back to 298.15 K assuming a linear log *K* versus 1/*T* behavior. Examination of the numerical values in Table 5 reveals that the Eqn. 18 provides reasonably accurate predictions of the partitioning behavior of the 60 organic solutes studied by Marciniak and Wlazlo. The average absolute deviation between the predicted and extrapolated experimental data was 0.16 log units, which is just slightly larger than the standard deviations in our derived log *K* correlations for [MeoeMPip]⁺[FAP]⁻. Past experience with the Abraham model has shown that IL-specific correlations (Eqns. 8 – 10) give slightly better predictions than correlations using the ion-specific equation coefficients (Eqn. 18). Predictions using the ion-specific equation coefficients are generally accurate enough for many practical applications, however, particularly in those instances where one does not have an IL-specific correlation expression to use.

4. References

- Hallet, J. P., Welton, T. *Chem. Rev.*, 2011, 111, 3508.
- Sowmiah, S., Cheng, C. I. Chu, Y.-H. *Curr. Org. Synth.*, 2012, 9, 74.
- Sandhu, S., Sandhu, J. S. *Green Chem. Lett. Review*, 2011, 4, 289.
- Sandhu, S., Sandhu, J. S. *Green Chem. Let. Review*, 2011, 4, 311.
- Yao, C., Anderson, J. L. *J. Chromatogr. A*, 2009, 1216, 1658.
- Poole, C. F., Poole, S. K. *J. Sep. Sci.*, 2011, 34, 888.
- Ragonese, C., Sciarone, D., Tranchida, Dugo, P., Mondello, L. *J. Chromatogr. A*, 2012, 1255, 130.
- Pino, V., Afonso, A. M. *Anal. Chim. Acta*, 2012, 714, 20.
- Vidal, L., Rickkola, M.-L., Canals, A. *Anal. Chim. Acta*, 2012, 715, 19.
- Ho, T. D., Canestralo, A. J., Anderson, J. L. *Anal. Chim. Acta*, 2011, 695, 18.
- Abraham, M. H. *Chem. Soc. Reviews*, 1993, 22, 73.
- Abraham, M. H., Ibrahim, A., Zissimos, A. M. *J. Chromatogr. A*, 2004, 1037, 29.
- Stephens, T. W., Loera, M., Quay, A. N., Chou, V., Shen, C., Wilson, A., Acree, W. E. Jr., Abraham, M. H. *Open Thermodyn. J.*, 2011, 5, 104.
- Abraham, M. H., Acree, W. E. Jr. *Thermochim. Acta*, 2011, 526 (2011).
- Saifullah, M., Ye, S., Grubbs, L. M., De La Rosa, N. E., Acree, W. E. Jr., Abraham, M. H. *J. Solution Chem.*, 2011, 40, 2082.
- Abraham, M. H., Smith, R. E., Luchtefeld, R., Boorem, A. J., Luo, R., Acree, W. E. Jr. *J. Pharm. Sci.*, 2010, 99, 1500.
- Stephens, T. W., De La Rosa, N. E., Saifullah, M., Ye, S., Chou, V., Quay, A. N., Acree, W. E. Jr., Abraham, M. H. *Fluid Phase Equilib.*, 2011, 309, 30.
- Stephens, T. W., De La Rosa, N. E., Saifullah, M., Ye, S., Chou, V., Quay, A. N., Acree, W. E. Jr., Abraham, M. H. *Fluid Phase Equilib.*, 2011, 308, 64.
- Acree, W. E. Jr., Abraham, M. H. *J. Chem. Technol. Biotechnol.*, 2006, 81, 1441 [Erratum: *J. Chem. Technol. Biotechnol.*, 2006, 81, 1722].
- Mintz, C., Acree, W. E. Jr. *Phys. Chem. Liq.*, 2007, 45, 241.
- Mutelet, F., Revelli, A.-L., Jaubert, J.-N., Sprunger, L. M., Acree, W. E. Jr., Baker, G. A. *J. Chem. Eng. Data*, 2010, 55, 234.
- Revelli, A.-L., Mutelet, F., Jaubert, J.-N., Garcia-Martinez, M., Sprunger, L. M., Acree, W. E. Jr., Baker, G. A. *J. Chem. Eng. Data*, 2010, 55, 2434.
- Grubbs, L. M., Ye, S., Saifullah, M., McMillan-Wiggins, M. C., Acree, W. E. Jr., Abraham, M. H., Twu, P., Anderson, J. L. *Fluid Phase Equilib.*, 2011, 301, 257.
- Proctor, A., Sprunger, L. M., Acree, W. E. Jr., Abraham, M. H. *Phys. Chem. Liq.*, 2008, 46, 631.
- Abraham, M. H., Acree, W. E. Jr. *Green Chem.*, 2006, 8, 906.
- Moise, J.-C., Mutelet, F., Jaubert, J.-N., Grubbs, L. M., Acree, W. E. Jr., Baker, G. A. *J. Chem. Eng. Data*, 2011, 56, 3106.
- Sprunger, L. M., Acree, W. E. Jr., Abraham, M. H. *Phys. Chem. Liq.*, 2010, 48, 394.
- Grubbs, L. M., Ye, S., Saifullah, M., Acree, W. E. Jr., Twu, P., Anderson, J. L., Baker, G. A., Abraham, M. H. *J. Solution Chem.*, 2011, 40, 2000.
- Sprunger, L. M., Gibbs, J., Baltazar, Q. Q., Acree, W. E. Jr., Abraham, M. H., Anderson, J. L. *Phys. Chem. Liq.*, 2009, 47, 74.
- Grubbs, L. M., Saifullah, M., De La Rosa, N. E. Acree, W. E. Jr., Abraham, M. H., Zhao, Q., Anderson, J. L. *Glob. J. Phys. Chem.*, 2010, 1, 1.
- Stephens, T. W., Acree, W. E. Jr., Twu, P., Anderson, J. L., Baker, G. A., Abraham, M. H. *J. Solution Chem.*, 2012, 41, 1165.
- Acree, W. E. Jr., Grubbs, L. M., Abraham, M. H., Selection of Ionic Liquid Solvents for Chemical Separations Based on the Abraham Model, in *Ionic Liquids: Applications and Perspectives* (Book 2), Kokorin, A. (Editor), INTECH Publishers, 2011, Chapter 13, 273.
- Revelli, A.-L., Sprunger, L. M., Gibbs, J., Acree, W. E. Jr., Baker, G. A., Mutelet, F. *J. Chem. Eng. Data*, 2009, 54, 977.
- Sprunger, L. M., Acree, W. E. Jr., Abraham, M. H. *Phys. Chem. Liq.*, 2010, 48, 385.

- ³⁵ Sprunger, L., Clark, M., Acree, W. E. Jr., Abraham, M. H. *J. Chem. Inf. Model.*, 2007, 47, 1123.
- ³⁶ Sprunger, L. M., Proctor, A., Acree, W. E. Jr., Abraham, M. H. *Fluid Phase Equilib.*, 2008, 265, 104.
- ³⁷ Sprunger, L. M., Gibbs, J., Proctor, A., Acree, W. E. Jr., Abraham, M. H., Meng, Y., Yao, C., Anderson, J. L. *Ind. Eng. Chem. Res.*, 2009, 48, 4145.
- ³⁸ Marciniak, A., Wlazlo, M. *J. Chem. Thermodyn.*, 2013, in press, [<http://dx.doi.org/10.1016/j.jct.2012.08.016>].
- ³⁹ Baltazar, Q. Q., Leininger, S. K., Anderson, J. L. *J. Chromatogr. A*, 2008, 1182, 119.
- ⁴⁰ Abraham, M. H., Andonian-Haftvan, J., Whiting, G. S., Leo, A., Taft, R. W. *J. Chem. Soc., Perkin Trans 2*, 1994, 1971.
- ⁴¹ Abraham, M. H., Ibrahim, A., Acree, W. E. Jr. *Fluid Phase Equilib.*, 2007, 251, 93.
- ⁴² Abraham, M. H., Ibrahim, A., Zissimos, A. M. *J. Chromatogr. A*, 2004, 1037, 29.
- ⁴³ Zissimos, A. M., Abraham, M. H., Barker, M. C., Box, K. J., Tam, K. Y., *J. Chem. Soc. Perkin Trans. 2*, 2002, 470.
- ⁴⁴ Zissimos, A. M., Abraham, M. H., Du, C. M., Valko, K., Bevan, C., Reynolds, D., Wood, J., Tam, K. Y., *J. Chem. Soc., Perkin Trans. 2*, 2002, 2001.
- ⁴⁵ Dohanvosova, P., Sarraute, S., Dohnal, V., Majer, V., Gomes, M. C. *Ind. Eng. Chem. Res.*, 2004, 43, 2805.
- ⁴⁶ Marciniak, A., Wlazlo, M. *J. Chem. Thermodyn.*, 2012, 49, 137.

Received: 30.09.2012.

Accepted: 04.10.2012.